THE JOURNAL OF PHYSICAL CHEMISTRY A

Article

pubs.acs.org/JPCA

Photocatalytic Oxygenation of 10-Methyl-9,10-dihydroacridine by O_2 with Manganese Porphyrins

Jieun Jung,[†] Kei Ohkubo,[†] David P. Goldberg,*[,‡] and Shunichi Fukuzumi*[,†]

[†]Department of Material and Life Science, Graduate School of Engineering, Osaka University and ALCA, Japan Science and Technology Agency (JST), 2-1 Yamada-oka, Suita, Osaka 565-0871, Japan

[‡]Department of Chemistry, The Johns Hopkins University, Baltimore, Maryland 21218, United States

Supporting Information

ABSTRACT: Photocatalytic oxygenation of 10-methyl-9,10-dihydroacridine ($AcrH_2$) by dioxygen (O_2) with a manganese porphyrin [(P)Mn^{III}: 5,10,15,20-tetrakis-(2,4,6-trimethylphenyl)-porphinatomanganese(III) hydroxide [(TMP)Mn^{III}(OH)] (**1**) or 5,10,15,20-tetrakis(pentafluorophenyl)porphyrinatomanganese-(III) acetate [(TPFPP)$Mn^{III}(CH_3COO)$] (**2**)] occurred to yield 10-methyl-(9,10*H*)-acridone (Acr═O) in an oxygen-saturated benzonitrile (PhCN) solution under visible light irradiation. The photocatalytic reactivity of (P)Mn^{III} in the presence of O_2 is in proportion to concentrations of $AcrH_2$ or O_2 with the maximum turnover numbers of 17 and 6 for **1** and **2**, respectively. The quantum yield with **1** was determined to be 0.14%. Deuterium kinetic isotope effects (KIEs) were observed with KIE = 22 for **1** and KIE = 6 for **2**, indicating that hydrogen-atom transfer from $AcrH_2$ is involved in the rate-determining step of the photocatalytic reaction. Femtosecond transient absorption measurements are consistent with photoexcitation of (P)Mn^{III}, resulting in intersystem crossing from a tripquintet excited state to a tripseptet excited state. A mechanism is proposed where the tripseptet excited state reacts with O_2 to produce a putative (P)Mn^{IV} superoxo complex. Hydrogen-atom transfer from $AcrH_2$ to (P)$Mn^{IV}(O_2^{\bullet-})$ generating a hydroperoxo complex (P)Mn^{IV}(OOH) and $AcrH^{\bullet}$ is likely the rate-determining step, in competition with back electron transfer to regenerate the ground state (P)Mn^{III} and O_2. The subsequent reductive O−O bond cleavage by $AcrH^{\bullet}$ may occur rapidly inside of the reaction cage to produce (P)Mn^{V}(O) and AcrH(OH), followed by the oxidation of AcrH(OH) by (P)Mn^{V}(O) to yield Acr═O with regeneration of (P)Mn^{III}.

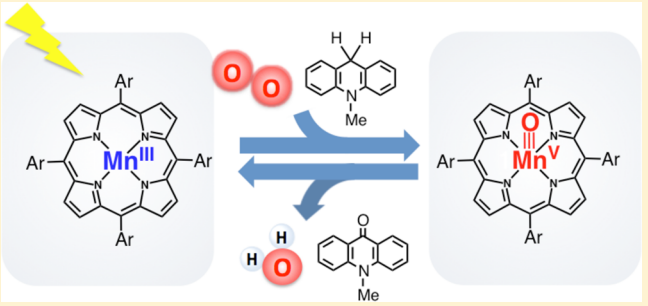

INTRODUCTION

High-valent metal−oxo complexes are the reactive oxidants in the oxidation of various substrates with heme and nonheme iron enzymes.[1−6] Synthetic high-valent metal−oxo complexes have been prepared using oxidants such as peroxy acids, iodosylarenes, and hydrogen peroxide, and the mechanisms of oxidation of substrates by high-valent metal−oxo complexes have been studied extensively.[7−12] High-valent metal−oxo complexes have also been produced by using dioxygen (O_2) with reductants.[13−18] Among various high-valent metal−oxo complexes, high-valent manganese−oxo complexes have attracted special attention because they are postulated as important intermediates for water oxidation in the oxygen-evolving center (OEC) of photosystem II.[19−27] A well-characterized manganese-(V)−oxo complex has been prepared by oxidation of a manganese(III) corrolazine [(TBP_8Cz)Mn^{III}; TBP_8Cz^{3-} = octakis-(*p*-*tert*-butylphenyl)corrolazinato^{3-}] with O_2 in the presence of toluene derivatives under visible light irradiation.[28,29] The (TBP_8Cz)Mn^{III} complex also acts as a photocatalyst for oxidation of 10-methyl-9,10-dihydroacridine ($AcrH_2$) by O_2.[29] However, there has been no report on photocatalytic oxidation of substrates by O_2 using manganese porphyrins.

We report herein the photocatalytic oxidation of $AcrH_2$ by O_2 with manganese(III) porphyrins [(P)Mn^{III}: (TMP)-Mn^{III}(OH) (**1**: TMP^{2-} = dianion of tetramesitylporphyrin) and (TPFPP)$Mn^{III}(CH_3COO)$ (**2**: $TPFPP^{2-}$ = dianion of 5,10,15,20-tetrakis(pentafluorophenyl)porphyrin)] (Chart 1) under visible light irradiation in O_2-saturated benzonitrile (PhCN) at room temperature. The photocatalytic reactivity of manganese porphyrin complexes is compared with that of (TBP_8Cz)Mn^{III}. The photocatalytic mechanism of oxidation of $AcrH_2$ by O_2 with (P)Mn^{III} is investigated based on kinetic studies and laser flash transient absorption measurements to clarify the photoinduced reaction mechanism of (P)Mn^{III} with O_2.

EXPERIMENTAL SECTION

Materials. The (TMP)Mn^{III}(OH) was synthesized according to published procedures.[30] The (TPFPP)$Mn^{III}(CH_3COO)$ complex was prepared by the following procedures. First, 5,10,15,20-tetrakis(pentafluorophenyl)porphyrin (0.10 g) from Sigma-Aldrich Co., manganese(II) acetate (0.96 g) from Wako Pure Chemical Industries, Ltd. and DMF (25 mL) were placed in a round-bottomed flask (50 mL). After the mixture was refluxed and stirred for 6 h, the solvent was removed under

Received: June 12, 2014
Revised: July 17, 2014
Published: July 18, 2014

   dx.doi.org/10.1021/jp505860f | *J. Phys. Chem. A* 2014, 118, 6223−6229

Chart 1. Manganese(III) Porphyrins Used in This Study

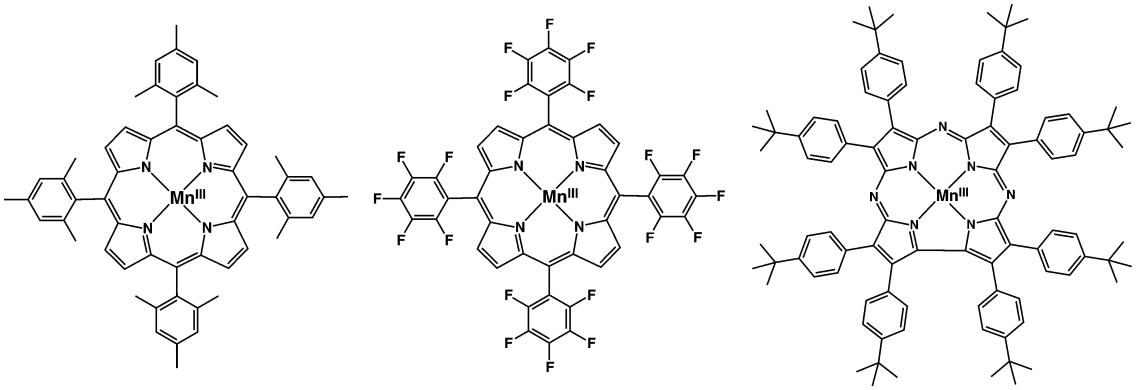

reduced pressure to yield 0.245 g of crude (TPFPP)-$Mn^{III}(CH_3COO)$ as a dark solid that was used without further purification. 10-Methyl-9,10-dihydroacridine ($AcrH_2$) was prepared by reduction of 10-methylacridinium perchlorate ($AcrH^+ClO_4^-$, Tokyo Chemical Industry Co., Ltd.) with $NaBH_4$.[31] PhCN was distilled over P_2O_5 in vacuo and stored under an argon atmosphere prior to use.[32]

Photocatalytic Reaction. The reactivity of photocatalytic oxygenation of manganese(III) complexes, **1** or **2** (1.0×10^{-5} M), with $AcrH_2$ and O_2 was evaluated by monitoring the UV−vis absorption spectral change in a quartz cuvette (10 mm × 10 mm). Visible light irradiation was carried out by a xenon lamp (500 W) through a transmitting glass filter (λ < 480 nm). In a typical experiment, **1** or **2** (1.0×10^{-5} M) was dissolved in PhCN (2.0 mL) containing $AcrH_2$ (0−2.0×10^{-1} M) in the quartz cuvette. The mixture was degassed by bubbling O_2 gas for 10 min, and then, the reaction was initiated by irradiating the solution with a xenon lamp transmitting through a color glass filter (λ > 480 nm). The electronic absorption spectral changes during photocatalytic oxygenation of **1** or **2** were monitored using a Hewlett−Packard HP8453 diode array spectrophotometer. The yield of Acr═O produced was calculated by an increase in the absorption band at 402 nm ($\varepsilon_{max} = 8.6 \times 10^3$ M^{-1} cm^{-1}) in PhCN due to Acr═O.[33]

Quantum Yield Determination. A standard actinometer (potassium ferrioxalate)[34] was used to estimate the quantum yield of the photochemical oxidation of **1** (1.0×10^{-5} M) with O_2 and $AcrH_2$ (0−1.5×10^{-1} M) in PhCN (2.0 mL). Typically, a square quartz cuvette (10 mm × 10 mm) that contained an O_2-saturated PhCN solution (2.0 mL) of **1** (1.0×10^{-5} M) and $AcrH_2$ was irradiated with a Panther OPO pumped Nd:YAG laser (Continuum, SLII-10, 4−6 ns fwhm) at λ = 476 nm. Typical pulse energies for the photoexcitation of the sample solution were in the range of 10 mJ per pulse. Under the conditions of actinometry experiments, the actinometer and **1** absorbed essentially all of the incident monochromatized light at 476 nm. The light intensity at 476 nm was 1.8×10^{-9} einstein s^{-1}. The quantum yields were estimated by monitoring the appearance of absorbance at 402 nm ($\varepsilon_{max} = 8.6 \times 10^3$ M^{-1} cm^{-1}) due to Acr═O.

Femtosecond Laser Flash Photolysis Measurements. Measurements of transient absorption spectra of **1** and **2** were carried out according to the following procedures. An O_2- or N_2-saturated PhCN solution containing **1** (4.0×10^{-5} M) or **2** (8.0×10^{-5} M) was excited by a femtosecond laser pulse at 393 nm using an ultrafast laser source, Integra-C (Quantronix Corp.), and a second harmonic generation (SHG) unit, Apollo (Ultrafast Systems, U.S.A). The optical detection system Helios was also provided by Ultrafast Systems. The detailed instrumental setting is shown in the Supporting Information.

Kinetic analyses were assembled from the time-resolved spectral data. The decay rate of the tripquintet ($^5T_1$) of manganese(III) porphyrin obeyed the first-order kinetics given by eq 1

$$\Delta Abs = A_1 \exp(-k_1 t) + A_2 \quad (1)$$

where A_1 is the pre-exponential factor for the absorption changes, A_2 is the final absorbance, and k_1 is the rate constant of the decay of the tripquintet ($^5T_1$) after femtosecond laser pulse irradiation. The slower decay rate of the tripseptet ($^7T_1$) also obeyed the first-order kinetics given by eq 2, where A_3 is the final absorbance at 565 nm and k_2 is the rate constant of the decay of $^7T_1$.

$$\Delta Abs = A_1 \exp(-k_1 t) + A_2 \exp(-k_2 t) + A_3 \quad (2)$$

RESULTS AND DISCUSSION

Photocatalytic Oxidation Reaction of $AcrH_2$ by O_2 with (P)Mn^{III}X. The photocatalytic oxidation of 10-methyl-9,10-dihydroacridine ($AcrH_2$) by O_2 with (P)Mn^{III}X was performed by photoirradiation of an O_2-saturated PhCN solution containing $AcrH_2$ and (TMP)Mn^{III}(OH) (**1**) or (TPFPP)-$Mn^{III}(CH_3COO)$ (**2**) using a xenon lamp (500 W) with a transmitting glass filter (λ > 480 nm). The absorption spectral changes in the photocatalytic oxidation of $AcrH_2$ by O_2 with **1** and **2** are shown in Figures 1a and b, respectively. The absorption spectra of **1** and **2** remained during the photocatalytic reaction, whereas the absorption band at λ_{max} = 402 nm ($\varepsilon_{max} = 8.6 \times 10^3$ M^{-1} cm^{-1}) due to 10-methyl-(9,10*H*)-acridone (Acr═O) appeared and the concentration of Acr═O increased linearly with photoirradiation time. The turnover numbers were determined to be 17 and 6 for **1** and **2** at 5 h of photoirradiation. It was confirmed that no formation of Acr═O was observed in the absence of O_2 or the light source [see Figures S1 and S2 in the Supporting Information (SI)]. It should be noted, however, that the direct photo-oxidation of $AcrH_2$ by O_2 occurred under photoirradiation without a glass filter.[35] The stoichiometry of the photocatalytic oxidation of $AcrH_2$ by O_2 is given by eq 3.

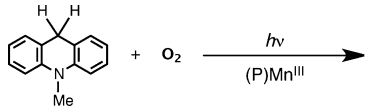

(3)

dx.doi.org/10.1021/jp505860f | J. Phys. Chem. A 2014, 118, 6223−6229

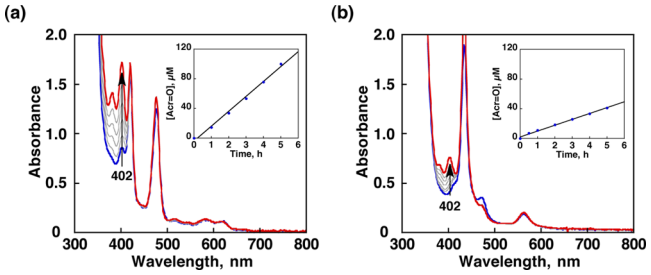

Figure 1. UV−vis absorption spectral changes and time course of formed Acr═O (inset) in an O_2-saturated PhCN solution (2.0 mL) containing (a) (TMP)Mn^{III}(OH) (1.0×10^{-5} M) or (b) (TPFPP)-Mn^{III}(CH_3COO) (1.0×10^{-5} M) and $AcrH_2$ (2.0×10^{-1} M) under visible light irradiation ($\lambda > 480$ nm).

Kinetics. Rates of formation of Acr═O in the photocatalytic oxidation of $AcrH_2$ with **1** in O_2-saturated PhCN were monitored by an appearance in the absorbance at 402 nm due to Acr═O under photoirradiation using a xenon lamp with a transmitting glass filter ($\lambda < 480$ nm) at 298 K. The initial reaction rate of the photocatalytic oxidation of $AcrH_2$ by O_2 in Figure 2a was determined to avoid the effects of changes in the

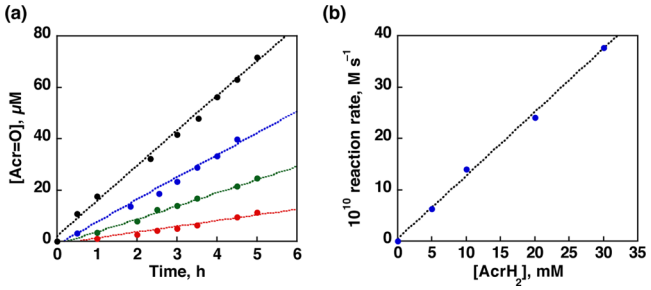

Figure 2. (a) Plots of the formation of Acr═O during the photocatalytic oxygenation of $AcrH_2$ under irradiation ($\lambda > 480$ nm) for an O_2-saturated PhCN solution containing (TMP)Mn^{III}(OH) (1.0×10^{-5} M) in the presence of 5 (red), 10 (green), 20 (blue), or 30 mM (black) of $AcrH_2$ as a substrate at 298 K. (b) Plot of the initial reaction rate versus concentration of $AcrH_2$.

light intensity absorbed by **1** and also in the concentration of $AcrH_2$.

The initial reaction rate increased with increasing concentration of $AcrH_2$, as shown in Figure 2b. The initial reaction rates are proportional to the concentration of O_2 (Figure 3). Thus, the rate law is given by eq 4, where k_{ox} is the second-

$$\frac{d[AcrH_2]}{dt} = k_{ox}[S][O_2] \quad (4)$$

order rate constant and [S] is the substrate concentration. The k_{ox} value was determined from the slope in Figure 2b to be 1.5×10^{-5} M^{-1} s^{-1} for **1** and 8.5×10^{-6} M^{-1} s^{-1} for **2** (Figures S3 in the SI).

The reaction solution of **1** (1.0×10^{-5} M) with O_2 and $AcrH_2$ (0−1.5×10^{-1} M) in O_2-saturated PhCN (2.0 mL) was irradiated to determine the quantum yield by changing the light source from a xenon lamp with a transmitting glass filter ($\lambda > 480$ nm) to nanosecond pulse where typical pulse energies at the sample were in the range of 10 mJ per pulse laser at 476 nm. The absorption band for Acr═O appeared, and the concentration of Acr═O increased linearly with excitation numbers. The zeroth-order rate constant of the photocatalytic

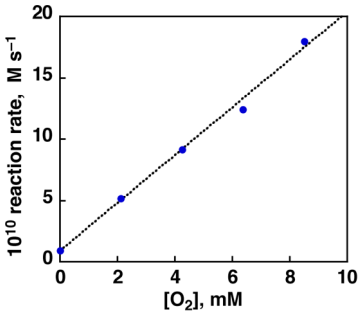

Figure 3. Plot of the initial reaction rate for the oxidation of (TMP)Mn^{III}(OH) (1.0×10^{-5} M) with O_2 (0−8.5×10^{-3} M)[36,37] and $AcrH_2$ (2.0×10^{-2} M) under photoirradiation by a xenon lamp ($\lambda > 480$ nm) versus the concentration of O_2 in PhCN at room temperature (298 K).

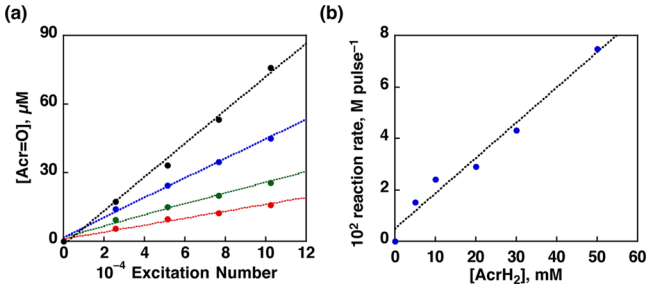

Figure 4. (a) Plots of the formation of Acr═O versus the laser excitation number for the photocatalytic oxygenation of $AcrH_2$ with an O_2-saturated PhCN solution containing (TMP)Mn^{III}(OH) (1.0×10^{-5} M) in the presence of 5.0 (red), 10 (green), 30 (blue), or 50 (black) of $AcrH_2$ as a substrate under irradiation by a nanosecond laser at 298 K. (b) Plot of the initial reaction rate versus concentration of $AcrH_2$.

oxidation of $AcrH_2$ by O_2 was also observed from the initial rate in Figure 4a. The quantum yield was determined to be 0.14% when **1** (1.0×10^{-5} M) with O_2 and $AcrH_2$ (1.5×10^{-1} M) in O_2-saturated PhCN (2.0 mL) was irradiated 1.0×10^5 times.

When $AcrH_2$ (0.20 M) was replaced by the dideuterated compound, $AcrD_2$, the reaction rate of formation of Acr═O became significantly slower with 22 or 6 as the deuterium kinetic isotope effect (KIE) values for **1** or **2**, as shown in Figure 5. The KIE value shows that the hydrogen-atom transfer

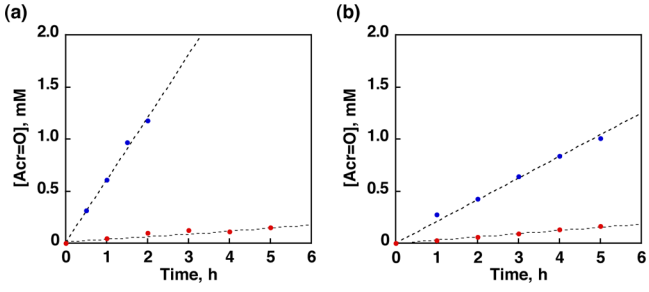

Figure 5. Time courses of Acr═O formed under photoirradiation ($\lambda > 480$ nm) of an O_2-saturated PhCN solution (0.5 mL) containing (a) **1** or (b) **2** (1.7×10^{-4} M) and $AcrH_2$ (blue, 0.20 M) or $AcrD_2$ (red, 0.20 M).

(HAT) from $AcrH_2$ is directly involved in the rate-determining step for the photocatalytic reaction of (P)Mn^{III} with O_2 and $AcrH_2$.

dx.doi.org/10.1021/jp505860f | J. Phys. Chem. A 2014, 118, 6223−6229

Femtosecond Transient Absorption Measurements. Femtosecond transient absorption spectroscopy was employed to investigate the photochemical processes involved in the photocatalytic oxygenation of $AcrH_2$ with $(P)Mn^{III}$ and O_2. Time-resolved transient absorption measurements by femtosecond laser flash photolysis of $(P)Mn^{III}$ were performed in the absence and presence of O_2 in PhCN. Figure 6a shows the transient absorption spectral change of **1** in N_2-saturated PhCN. Femtosecond laser excitation at 393 nm resulted in an instantaneous appearance of an absorption maximum at λ_{max} = 638 nm, which is assigned to the tripquintet excited state ($^5T_1$). It has been reported that the Mn^{III} metal ion has a d^4 ground-state electronic configuration ($S = 2$).[29,38] Therefore, the (π,π^*) states of $(P)Mn^{III}$ are not the normal singlets or triplets because of coupling of the unpaired metal electrons with the ring π electrons of the corrolazine ring. The ground state is a quintet ($^5S_0$), and a quintet excited state ($^5S_1$) is derived from the lowest excited ring (π,π^*) singlet.[29,38] The excited states of first-row paramagnetic complexes, such as Mn^{III} complexes, undergo an extremely rapid intersystem crossing (ISC) process from the quintet ($^5S_1$) excited state to the tripquintet ($^5T_1$) excited state.[38−42] The transient absorption spectra in Figure 6a show the decay of the absorption band at 638 nm, indicating ISC from the tripquintet ($^5T_1$) state to the long-lived tripseptet ($^7T_1$) state, which has an absorption band at 565 nm. From the decay profile of the tripquintet ($^5T_1$), a rate constant of 2.3×10^{10} s^{-1} obeying first-order kinetics in degassed PhCN (Figure 6b) was determined. The rate constant of 2.5×10^{10} s^{-1} was also determined in aerated PhCN (Figure 6c), indicating no oxygen dependence on the rate of ISC.

The absorbance at 565 nm due to $^7T_1$ was diminished faster in O_2-saturated PhCN (Figure 6e) rather than in deaerated PhCN (Figure 6d), providing a direct reaction between the excited state and O_2. The second-order rate constant of the decay of $[(TMP)Mn^{III}(OH)]^*$ ($^7T_1$) in the presence of O_2 was determined to be $(8.1 \pm 2.0) \times 10^9$ M^{-1} s^{-1}, which is comparable to the diffusion-limited rate constant in PhCN (5.6×10^9 M^{-1} s^{-1}).[43] The fast absorbance decay for $^7T_1$ also occurred when $(P)Mn^{III}$ replaced from **1** to **2** (Figure S4 in the SI) with 2.0×10^7 M^{-1} s^{-1} of the second-order rate constant of the decay of $[(TPFPP)Mn^{III}(CH_3COO)]^*$ ($^7T_1$). Together with the second-order rate constant of the decay of $[(TBP_8Cz)Mn^{III}]^*$ ($^7T_1$), which is 4.9×10^9 M^{-1} s^{-1},[29] the second-order rate constants of the decay of $[Mn^{III}]^*$ ($^7T_1$) corresponding to the rate constant of bimolecular reaction between $[Mn^{III}]^*$ ($^7T_1$) and O_2 increased in the order of $(TMP)Mn^{III}(OH)$, $(TBP_8Cz)Mn^{III}$, and $(TPFPP)Mn^{III}(CH_3COO)$. This order agrees with the order of the maximum turnover number of photocatalytic oxidation of $AcrH_2$ in the presence of Mn^{III} in O_2-saturated PhCN under photoirradiation.

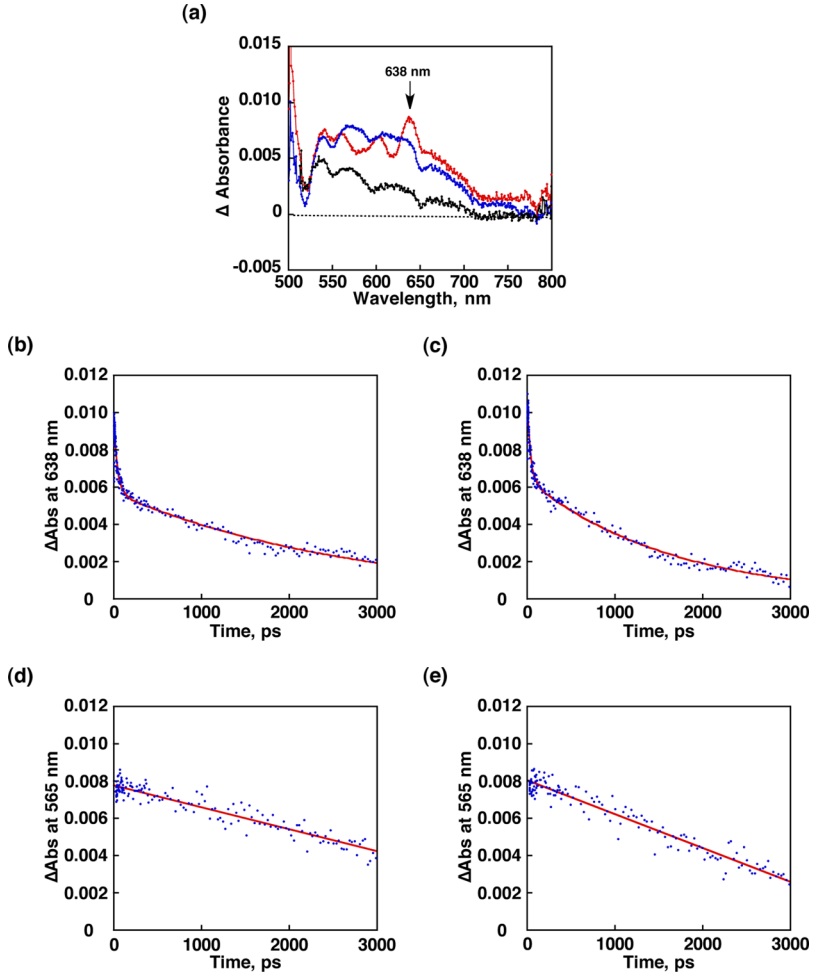

Figure 6. (a) Transient absorption spectral changes (red after 10 ps, blue 50 ps, and black 3000 ps) after photoexcitation of $(TMP)Mn^{III}(OH)$ in PhCN. Decay time profiles of absorbance at 638 nm due to $[(TMP)Mn^{III}(OH)]^*$ ($^5T_1$) (b) in N_2-saturated PhCN and (c) in O_2-saturated PhCN. Decay time profiles of absorbance due to $[(TMP)Mn^{III}(OH)]^*$ ($^7T_1$) at λ = 565 nm under (d) N_2 and (e) O_2.

dx.doi.org/10.1021/jp505860f | J. Phys. Chem. A 2014, 118, 6223−6229

Porphyrins and metalloporphyrins are well-known to be effective triplet-state photosensitizers and to be capable of producing singlet oxygen ($^1O_2$*) due to direct energy transfer from the porphyrin excited triplet state to molecular oxygen. To examine a role for singlet oxygen in this photochemistry, the possibility of generation of $^1O_2$* has been examined by comparison of $^1O_2$* phosphorescence spectra in the presence of (P)Mn^{III} or C_{60}. The photoexcitation of (P)Mn^{III} with light of λ = 532 nm in O_2-saturated deuterated benzene (C_6D_6) results in a negligible phosphorescence signal at 1270 nm,[44] which is the phosphorescence spectrum of $^1O_2$*, whereas that obtained by photoirradiation of C_{60} under the same conditions shows significantly intense spectra, as shown in Figure S5 in the SI. Thus, it was assessed that the contribution of $^1O_2$* for the photochemical oxidation of (P)Mn^{III} with O_2 may be negligible as compared with an electron-transfer pathway from [(P)Mn^{III}]* ($^7T_1$) to O_2. It has been revealed that a significant role for $^1O_2$* was ruled out upon the photochemical oxidation of (TBP_8Cz)Mn^{III} to (TBP_8Cz)Mn^{V}(O) by use of a $^1O_2$* trap reagent, 9,10-dimethylanthracene.[29]

Photocatalytic Mechanism. The mechanism of photocatalytic oxidation of $AcrH_2$ by O_2 with (P)Mn^{III} to give Acr═O as the product is proposed according to the photodynamics of (P)Mn^{III}, together with the large KIE values, as shown in Scheme 1. After photoexcitation of (P)Mn^{III}, the tripquintet

Scheme 1. Mechanism of Photocatalytic Oxidation of $AcrH_2$ in the Presence of (P)Mn^{III} and O_2

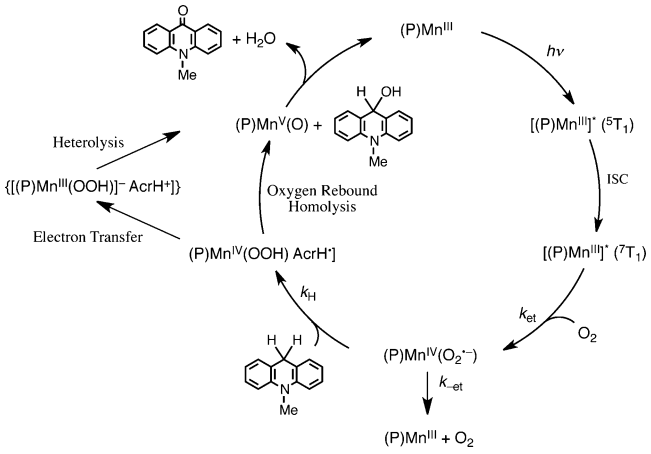

excited state ([(P)Mn^{III}]* ($^5T_1$)) is produced and converted rapidly to the triplet excited state ([(P)Mn^{III}]* ($^7T_1$)) by ISC. Generated [(P)Mn^{III}]* ($^7T_1$) undergoes electron transfer from [(P)Mn^{III}]* ($^7T_1$) to O_2 to produce the superoxo complex [(P)Mn^{IV}($O_2^{\bullet-}$)], followed by HAT from $O_2^{\bullet-}$ moiety to the (P)Mn^{IV} to produce the hydroperoxo complex (P)Mn^{IV}(OOH) and acridinyl radical ($AcrH^{\bullet}$), which is the rate-determining step of the overall reaction. This reaction is most likely in competition with the back electron transfer from $O_2^{\bullet-}$ moiety to the (P)Mn^{IV} to regenerate the ground state of (P)Mn^{III} and O_2. The subsequent O−O bond cleavage by $AcrH^{\bullet}$ may occur rapidly inside of the reaction cage before the reaction of $AcrH^{\bullet}$ with O_2 to yield (P)Mn^{V}(O) and 9-hydroxy-10-methyl-9,10-dihydroacridine [AcrH(OH)]. This is followed by subsequent facile oxidation of AcrH(OH) by (P)Mn^{V}(O) to yield Acr═O, accompanied by regeneration of (P)Mn^{III} (Scheme 1).

When the hydrogen transfer from $AcrH_2$ to (P)Mn^{IV}($O_2^{\bullet-}$) is the rate-determining step in the catalytic cycle in Scheme 1, the rate of formation of Acr═O is given by eq 5, where k_H is the rate of HAT from $AcrH_2$ to (P)Mn^{IV}($O_2^{\bullet-}$).

$$\frac{d[Acr{=}O]}{dt} = k_H[AcrH_2][(P)Mn^{IV}(O_2^{\bullet-})] \quad (5)$$

The rate of formation and decay of (P)Mn^{IV}($O_2^{\bullet-}$) is given by eq 6

$$\frac{d[(P)Mn^{IV}(O_2^{\bullet-})]}{dt} = k_{et}[^7T_1][O_2] - k_H[AcrH_2][(P)Mn^{IV}(O_2^{\bullet-})] - k_{-et}[(P)Mn^{IV}(O_2^{\bullet-})] \quad (6)$$

where k_{et} is the rate constant of electron transfer from [(P)Mn^{III}]* ($^7T_1$) to O_2 to produce (P)Mn^{IV}($O_2^{\bullet-}$) and k_{-et} is the back electron transfer from the $O_2^{\bullet-}$ moiety to the (P)Mn^{IV} moiety to regenerate (P)Mn^{III} and O_2. The rate of formation and decay of $^7T_1$ is given by eq 7

$$\frac{d[^7T_1]}{dt} = \Phi_0 In - k_{et}[^7T_1][O_2] - k_2[^7T_1] \quad (7)$$

where Φ_0 is the quantum yield of formation of $^7T_1$, In is the light intensity absorbed by **1**, and k_2 is the decay rate constant of $^7T_1$ without O_2. By applying the steady-state approximation, the steady-state concentration of $^7T_1$ is derived from eq 7, as shown by eq 8

$$[^7T_1] = \frac{\Phi_0 In}{(k_{et}[O_2] + k_2)} \quad (8)$$

The steady-state concentration of Mn^{IV}($O_2^{\bullet-}$) is also derived from eqs 6 and 8, as given by eq 9

$$[(P)Mn^{IV}(O_2^{\bullet-})] = \frac{\Phi_0 In k_{et}[O_2]}{[(k_{-et} + k_H[AcrH_2])(k_2 + k_{et}[O_2])]} \quad (9)$$

Then, the quantum yield for photocatalytic oxidation of $AcrH_2$ is derived from eqs 5 and 9, as given by eq 10

$$\Phi = \frac{\Phi_0 k_H k_{et}[AcrH_2][O_2]}{[(k_{-et} + k_H[AcrH_2])(k_2 + k_{et}[O_2])]} \quad (10)$$

Equation 10 is rewritten by eq 11

$$\Phi^{-1} = \Phi_0^{-1}\left[\left(\frac{k_H}{k_{-et}}\right)^{-1}[AcrH_2]^{-1} + 1\right]\left[\left(\frac{k_{et}}{k_2}\right)^{-1}[O_2]^{-1} + 1\right] \quad (11)$$

where there are linear correlations for Φ^{-1} versus $[AcrH_2]^{-1}$ and Φ^{-1} versus $[O_2]^{-1}$. Linear plots of Φ^{-1} versus $[AcrH_2]^{-1}$ and Φ^{-1} versus $[O_2]^{-1}$ are shown in Figure 7a and b,

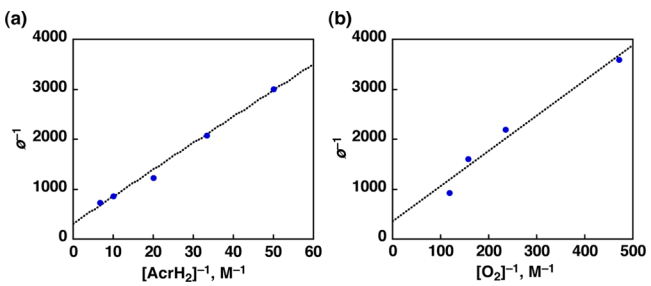

Figure 7. Linear plots of Φ^{-1} versus $[AcrH_2]^{-1}$ and Φ^{-1} versus $[O_2]^{-1}$.

dx.doi.org/10.1021/jp505860f | J. Phys. Chem. A 2014, 118, 6223−6229

respectively. From the slopes and intercepts of the linear plots, the k_H/k_{-et} and k_{et}/k_2 values were obtained as 53 and 7, respectively.

CONCLUSIONS

Photocatalytic oxidation of $AcrH_2$ by O_2 with (P)Mn^{III} (**1** and **2**) in PhCN occurs to produce Acr=O as the sole oxidation product. The kinetic and laser flash photolysis measurements revealed the photocatalytic mechanism, as shown in Scheme 1, where electron transfer from the excited state ($[(P)Mn^{III}]^*$ ($^7T_1$)) to O_2 occurs to produce the superoxo complex $[(P)Mn^{IV}(O_2^{\bullet-})]$, which oxidizes $AcrH_2$ to Acr=O via hydrogen-atom transfer from $AcrH_2$ to $[(P)Mn^{IV}(O_2^{\bullet-})]$ and formation of $(P)Mn^{V}(O)$. The photocatalytic reactivity of $(P)Mn^{III}$ agrees with the rate constants of electron transfer from $[(P)Mn^{III}]^*$ ($^7T_1$) to O_2 in the order $(TMP)Mn^{III}(OH)$ > $(TBP_8Cz)Mn^{III}$ > $(TPFPP)Mn^{III}(CH_3COO)$. The present study paves the way for development of new photocatalytic oxidation of substrates by O_2 using manganese porphyrins.

ASSOCIATED CONTENT

Supporting Information

Kinetic data (Figures S1, S2, and S3), femtosecond laser flash photolysis measurements (Figure S4), and phosphorescence spectra (Figure S5). This material is available free of charge via the Internet at http://pubs.acs.org.

AUTHOR INFORMATION

Corresponding Authors

*E-mail: fukuzumi@chem.eng.osaka-u.ac.jp (S.F.).
*E-mail: dpg@jhu.edu (D.P.G.).

Notes

The authors declare no competing financial interest.

ACKNOWLEDGMENTS

This work was supported by an ALCA project from the Japan Science and Technology Agency (JST), Japan to S.F., Grants-in-Aid (Nos. 26620154 and 26288037 to K.O.) from the Ministry of Education, Culture, Sports, Science, and Technology (MEXT), Japan, the NSF (CHE0909587 and CHE121386 to D.P.G.), and the NIH (GM101153 to D.P.G)

REFERENCES

(1) Rittle, J.; Green, M. T. Cytochrome P450 Compound I: Capture, Characterization, and C−H Bond Activation Kinetics. *Science* **2010**, *330*, 933−937.
(2) *Metal−oxo and Metal−Peroxo Species in Catalytic Oxidations*; Meunier, B., Ed.; Springer-Verlag: Berlin, Germany, 2000.
(3) *Cytochrome P450: Structure, Mechanism, and Biochemistry*, 3rd ed.; Ortiz de Montellano, P. R., Ed.; Kluwer Academic/Plenum Publishers: New York, 2005.
(4) Hrycay, E. G.; Bandiera, S. M. The Monooxygenase, Peroxidase, and Peroxygenase Properties of Cytochrome P450. *Arch. Biochem. Biophys.* **2012**, *522*, 71−89.
(5) Betley, T. A.; Wu, Q.; Voorhis, T. V.; Nocera, D. G. Electronic Design Criteria for O−O Bond Formation via Metal−Oxo Complexes. *Inorg. Chem.* **2008**, *47*, 1849−1861.
(6) Mullins, C. S.; Pecoraro, V. L. Reflections on Small Molecule Manganese Models that Seek to Mimic Photosynthetic Water Oxidation Chemistry. *Coord. Chem. Rev.* **2008**, *252*, 416−443.
(7) Hong, S.; Lee, Y.-M.; Shin, W.; Fukuzumi, S.; Nam, W. Dioxygen Activation by Mononuclear Nonheme Iron(II) Complexes Generates Iron−Oxygen Intermediates in the Presence of an NADH Analogue and Proton. *J. Am. Chem. Soc.* **2009**, *131*, 13910−13911.
(8) Nishida, Y.; Lee, Y.-M.; Nam, W.; Fukuzumi, S. Autocatalytic Formation of an Iron(IV)−Oxo Complex via Scandium Iron−Promoted Radical Chain Autoxidation of an Iron(II) Complex with Dioxygen and Tetraphenylborate. *J. Am. Chem. Soc.* **2014**, *136*, 8042−8049.
(9) Shen, D.; Miao, C.; Wang, S.; Xia, C.; Sun, W. Efficient Benzylic and Aliphatic C−H Oxidation with Selectivity for Methylenic Sites Catalyzed by a Bioinspired Manganese Complex. *Org. Lett.* **2014**, *16*, 1108−1111.
(10) Sorokin, A. B. Phthalocyanine Metal Complexes in Catalysis. *Chem. Rev.* **2013**, *113*, 8152−8191.
(11) Fukuzumi, S.; Kishi, T.; Kotani, H.; Lee, Y.-M.; Nam, W. Highly Efficient Photocatalytic Oxygenation Reactions Using Water as an Oxygen Source. *Nat. Chem.* **2011**, *3*, 38−41.
(12) Paria, S.; Chatterjee, S.; Paine, T. K. Reactivity of an Iron−Oxygen Oxidant Generated upon Oxidative Decarboxylation of Biomimetic Iron(II) α-Hydroxy Acid Complexes. *Inorg. Chem.* **2014**, *53*, 2810−2821.
(13) Company, A.; Sabenya, G.; González-Béjar, M.; Gómez, L.; Clémancey, M.; Blondin, G.; Jasniewski, A. J.; Puri, M.; Browne, W. R.; Latour, J.-M.; et al. Triggering the Generation of an Iron(IV)−Oxo Compound and Its Reactivity toward Sulfides by Ru^{II} Photocatalysis. *J. Am. Chem. Soc.* **2014**, *136*, 4624−4633.
(14) Li, F.; Van Heuvelen, K. M.; Meier, K. K.; Münck, E.; Que, L., Jr. Sc^{3+}-Triggered Oxoiron(IV) Formation from O_2 and Its Non-Heme Iron(II) Precursor via a Sc^{3+}−Peroxo−Fe^{3+} Intermediate. *J. Am. Chem. Soc.* **2013**, *135*, 10198−10121.
(15) Kim, S. O.; Sastri, C. V.; Seo, M. S.; Kim, J.; Nam, W. Dioxygen Activation and Catalytic Aerobic Oxidation by a Mononuclear Nonheme Iron(II) Complex. *J. Am. Chem. Soc.* **2005**, *127*, 4178−4179.
(16) Lee, Y.-M.; Hong, S.; Morimoto, Y.; Shin, W.; Fukuzumi, S.; Nam, W. Dioxygen Activation by a Non-Heme Iron(II) Complex: Formation of an Iron(IV)−Oxo Complex via C−H Activation by a Putative Iron(III)−Superoxo Species. *J. Am. Chem. Soc.* **2010**, *132*, 10668−10670.
(17) Hong, S.; Lee, Y.-M.; Shin, W.; Fukuzumi, S.; Nam, W. Dioxygen Activation by Mononuclear Nonheme Iron(II) Complexes Generates Iron−Oxygen Intermediates in the Presence of an NADH Analogue and Proton. *J. Am. Chem. Soc.* **2009**, *131*, 13910−13911.
(18) O'Reilly, M. E.; Del Castillo, T. J.; Falkowski, J. M.; Ramachandran, V.; Pati, M.; Correia, M. C.; Abboud, K. A.; Dalal, N. S.; Richardson, D. E.; Veige, A. S. Autocatalytic O_2 Cleavage by an OCO^{3-} Trianionic Pincer Cr^{III} Complex: Isolation and Characterization of the Autocatalytic Intermediate $[Cr^{IV}]_2(\mu$-O) Dimer. *J. Am. Chem. Soc.* **2011**, *133*, 13661−13673.
(19) McEvoy, J. P.; Brudvig, G. W. Water-Splitting Chemistry of Photosystem II. *Chem. Rev.* **2006**, *106*, 4455−4483.
(20) Umena, Y.; Kawakami, K.; Shen, J. R.; Kamiya, N. Crystal Structure of Oxygen-Evolving Photosystem II at a Resolution of 1.9 Å. *Nature* **2011**, *473*, 55−60.
(21) Pecoraro, V. L.; Baldwin, M. J.; Caudle, M. T.; Hsieh, W.-Y.; Law, N. A. A Proposal for Water Oxidation in Photosystem II. *Pure Appl. Chem.* **1998**, *70*, 925−929.
(22) Fukuzumi, S.; Fujioka, N.; Kotani, H.; Ohkubo, K.; Lee, Y.-M.; Nam, W. Mechanistic Insights into Hydride-Transfer and Electron-Transfer Reactions by a Manganese(IV)−Oxo Porphyrin Complex. *J. Am. Chem. Soc.* **2009**, *131*, 17127−17134.
(23) Arunkumar, C.; Lee, Y.-M.; Lee, J. Y.; Fukuzumi, S.; Nam, W. Hydrogen-Atom Abstraction Reactions by Manganese(V)− and Manganese(IV)−Oxo Porphyrin Complexes in Aqueous Solution. *Chem.—Eur. J.* **2009**, *15*, 11482−11489.
(24) Lee, J. Y.; Lee, Y.-M.; Kotani, H.; Nam, W.; Fukuzumi, S. High-Valent Manganese(V)−Oxo Porphyrin Complexes in Hydride Transfer Reactions. *Chem. Commun.* **2009**, 704−706.
(25) Prokop, K. A.; de Visser, S. P.; Goldberg, D. P. Unprecedented Rate Enhancements of Hydrogen-Atom Transfer to a Manganese(V)−Oxo Corrolazine Complex. *Angew. Chem.* **2010**, *122*, 5217−5221; *Angew. Chem., Int. Ed.* **2010**, *49*, 5091−5095.

(26) Fukuzumi, S.; Kotani, H.; Prokop, K. A.; Goldberg, D. P. Electron- and Hydride-Transfer Reactivity of an Isolable Manganese(V)−Oxo Complex. *J. Am. Chem. Soc.* **2011**, *133*, 1859−1869.
(27) Han, Y.; Lee, Y.-M.; Mariappan, M.; Fukuzumi, S.; Nam, W. Manganese(V)−Oxo Corroles in Hydride-Transfer Reactions. *Chem. Commun.* **2010**, *46*, 8160−8162.
(28) Prokop, K. A.; Goldberg, D. P. Generation of an Isolable, Monomeric Manganese(V)−Oxo Complex from O_2 and Visible Light. *J. Am. Chem. Soc.* **2012**, *134*, 8014−8017.
(29) Jung, J.; Ohkubo, K.; Prokop, K. A.; Neu, H. M.; Goldberg, D. P.; Fukuzumi, S. Photochemical Oxidation of a Manganese(III) Complex with Oxygen and Toluene Derivatives to Form a Manganese(V)−Oxo Complex. *Inorg. Chem.* **2013**, *52*, 13594−13604.
(30) Groves, J. T.; Stern, M. K. Synthesis, Characterization, and Reactivity of Oxomanganese(IV) Porphyrin Complexes. *J. Am. Chem. Soc.* **1988**, *110*, 8628−8638.
(31) Fukuzumi, S.; Ohkubo, K.; Tokuda, Y.; Suenobu, T. Hydride Transfer from 9-Substituted 10-Methyl-9,10-dihydroacridines to Hydride Acceptors via Charge-Transfer Complexes and Sequential Electron−Proton−Electron Transfer. A Negative Temperature Dependence of the Rates. *J. Am. Chem. Soc.* **2000**, *122*, 4286−4294.
(32) *Purification of Laboratory Chemicals*; Armarego, W. L. F., Perrin, D. D., Eds.; Pergamon Press: Oxford, U.K., 1997.
(33) Fukuzumi, S.; Ohkubo, K. Fluorescence Maxima of 10-Methylacridone−Metal Ion Salt Complexes: A Convenient and Quantitative Measure of Lewis Acidity of Metal Ion Salts. *J. Am. Chem. Soc.* **2002**, *124*, 10270−10271.
(34) Hatchard, C. G.; Parker, C. A. A New Sensitive Chemical Actinometer. II. Potassium Ferrioxalate as a Standard Chemical Actinometer. *Proc. R. Soc. London, Ser. A* **1956**, *235*, 518−536.
(35) Fukuzumi, S.; Ishikawa, M.; Tanaka, T. Mechanisms of Photo-oxidation of NADH Model Compounds by Oxygen. *J. Chem. Soc., Perkin Trans. 2* **1989**, 1037−1044.
(36) Fukuzumi, S.; Okamoto, K.; Gros, C. P.; Guilard, R. Mechanism of Four-Electron Reduction of Dioxygen to Water by Ferrocene Derivatives in the Presence of Perchloric Acid in Benzonitrile, Catalyzed by Cofacial Dicobalt Porphyrins. *J. Am. Chem. Soc.* **2004**, *126*, 10441−10449.
(37) Devoille, A. M. J.; Love, J. B. Double-Pillared Cobalt Pacman Complexes: Synthesis, Structures and Oxygen Reduction Catalysis. *Dalton Trans.* **2012**, *41*, 65−72.
(38) Kim, Y.; Choi, J. R.; Yoon, M. Excited-State Dynamics of 5,10,15,20-Tetraphenyl- 21*H*,23*H*-porphine Manganese(III) Chloride Encapsulated in TiMCM-41 and MCM-41; Proved by fs-Diffuse Reflectance Laser Photolysis. *J. Phys. Chem. B* **2001**, *105*, 8513−8518.
(39) Humphrey, J. L.; Kuciauskas, D. Charge Transfer Enhances Two-Photon Absorption in Transition Metal Porphyrins. *J. Am. Chem. Soc.* **2006**, *128*, 3902−3903.
(40) Spänig, F.; Ruppert, M.; Dannhäuser, J.; Hirsch, A.; Guldi, D. M. *trans-2* Addition Pattern to Power Charge Transfer in Dendronized Metalloporphyrin C_{60} Conjugates. *J. Am. Chem. Soc.* **2009**, *131*, 9378−9388.
(41) Gonçalves, P. J.; De Boni, L.; Borissevitch, I. E.; Zílio, S. C. Excited State Dynamics of *meso*-Tetra(sulphonatophenyl)-Metalloporphyrins. *J. Phys. Chem. A* **2008**, *112*, 6522−6526.
(42) Krokos, E.; Spänig, F.; Ruppert, M.; Hirsch, A.; Guldi, D. M. A Charge-Transfer Challenge: Combining Fullerenes and Metalloporphyrins in Aqueous Environments. *Chem.—Eur. J.* **2012**, *18*, 1328−1341.
(43) Kawashima, Y.; Ohkubo, K.; Fukuzumi, S. Small Reorganization Energies of Photoinduced Electron Transfer between Spherical Fullerenes. *J. Phys. Chem. A* **2013**, *117*, 6737−6743.
(44) Kashiwagi, Y.; Imahori, H.; Araki, Y.; Ito, O.; Yamada, K.; Sakata, Y.; Fukuzumi, S. Strong Inhibition of Singlet Oxygen Sensitization in Pyridylferrocene−Fluorinated Zinc Porphyrin Supramolecular Complexes. *J. Phys. Chem. A* **2003**, *107*, 5515−5522.